Preparation and Properties of Acid-Treated Multiwalled Carbon Nanotube/Waterborne Polyurethane Nanocomposites

Ji-Yun Kwon, Han-Do Kim

Department of Textile Engineering, Pusan National University, Busan 609–735, Korea

Received 1 June 2004; accepted 10 October 2004
DOI 10.1002/app.21436
Published online in Wiley InterScience (www.interscience.wiley.com).

ABSTRACT: Nitric acid treated multiwalled carbon nanotubes (A-CNTs) were dispersed in a waterborne polyurethane (WBPU) matrix to obtain WBPU/A-CNT nanocomposite films (99.99/0.01–98.5/1.5) with enhanced thermal, mechanical, and electrical properties. By X-ray photoelectron spectroscopy (XPS), the oxygen content of the carbon nanotube (CNT) surface was found to increase with increasing acid treatment time. With increasing acid treatment time, the contact angle of the CNT surface was significantly decreased from 15 to 0°. The mean particle sizes of the raw CNT and A-CNT aqueous solutions were 404.2 and 17.2 nm, respectively, indicating that the acid treatment led to a reduced agglomeration of CNTs. The electrical conductivity of raw CNT was 23 S/cm, and that of A-CNT significantly increased with increasing acid treatment time up to 30 min and then decreased a little. By dynamic mechanical thermal analysis, the storage modulus and loss tangent peak temperature (the glass-transition temperature) of the WBPU/A-CNT nanocomposites were found to increase with increasing A-CNT content. The initial tensile moduli and tensile strengths of the nanocomposite film with 1.5 wt % loading of A-CNT were enhanced by about 19 and 12%, respectively, compared to the corresponding values for the original WBPU film. The WBPU/A-CNT1.5 nanocomposite film containing 1.5 wt % of A-CNT exhibited a conductivity of 1.2 $\times$ 10^{-4} S/cm, which was nearly eight orders of magnitude higher that of the WBPU film (2.5 $\times$ 10^{-12} S/cm). The antistatic half-life ($\tau_{1/2}$) of the WBPU film was about 110 s, indicating that pure the WBPU film was a typical electrostatic material. However, those of the WBPU/A-CNT nanocomposites decreased exponentially with increasing A-CNT content. The WBPU/A-CNT1.5 sample, containing 1.5 wt % of A-CNT and with a $\tau_{1/2}$ of 1 s, had good antistatic properties. J Appl Polym Sci 96: 595–604, 2005

Key words: polyurethanes; nanocomposites; reinforcement

INTRODUCTION

Since the discovery of carbon nanotubes (CNTs)[1] and their novel mechanical and electrical properties,[2–4] extensive research in the field of CNT/polymer nanocomposites has begun. Some experimental studies on CNT-reinforced polymer materials have been reported for various kinds of organic polymers, including polyethylene,[5,6] polypropylene,[7] poly(methyl methacrylate),[8–10] pitch,[11] epoxy,[12–14] polystyrene,[15] and polyurethane,[16] with enhanced mechanical and electrical properties.

When CNTs are composed of one graphite sheet, they are called *single-walled CNTs*, and when they consist of more than one graphite sheet, they are called multiwalled carbon nanotubes (MWCNTs).[17] MWCNTs, which were the first type and which were found in 1991, have thicker walls consisting of several coaxial graphite cylinders separated by spacing (0.34 nm) that is close to the interlayer distance in graphite.[17,18] The CNTs can offer a kind of nanosize reinforcement with a light weight, a hollow-core immerse aspect ratio, and an exceptionally high axial strength.[4]

The nonreactive surface of the CNTs limits its applications in composites because of the lack of adhesion between CNTs and various matrix polymers. Intrinsic van der Waals attraction among tubes, in combination with their high surface area and high aspect ratio, often leads to significant agglomeration, thus preventing efficient transfer of their superior properties to the matrix.[10,19,20] The effective utilization of CNTs in nanocomposite applications depends strongly on the ability to disperse the CNTs homogeneously throughout the matrix without destroying the integrity of the CNTs.[5] Although a number of studies have focused on dispersion of CNTs, complete dispersion of CNTs in a polymer matrix has rarely been achieved. Most dispersion studies have been directed toward chemical modification of the CNT surface, such as through acid treatment and the incorporation of functional groups.[4,8,10,21–24]

Waterborne polyurethanes (WBPUs) are nontoxic and nonflammable and do not pollute the air. In ad-

Correspondence to: H.-D. Kim (kimhd@pusan.ac.kr).

TABLE I
Sample Designation and Composition of Waterborne Polyurethane (WBPU)

Sample designation	Composition (mole)					Solid content (wt %)
	IPDI	PTMG (Mn = 2,000)	DMPA	EDA	TEA	
WBPU	2.5	1.0	0.5	1.0	0.5	30

dition, water dispersion (emulsions) of WBPUs permit the application of polyurethane from an aqueous medium. WBPUs have been used for a wide range of commercial applications, including adhesives and coatings for various substrates.[25–29] However, WBPU/MWCNT nanocomposites have not been reported.

In this study, nitric acid treated multiwalled carbon nanotubes (A-CNTs) were used to improve the dispersability of CNTs in the WBPU matrix, and we focused on nanocomposites with low loadings of A-CNTs (0.01–1.5 wt %) because this provided a case for good dispersion of A-CNTs in the WBPU matrix.

A series of nanocomposite films of WBPU/A-CNT (99.99/0.01–98.5/1.5 wt %) were prepared by solution blending/casting from aqueous WBPU/A-CNT nanocomposites. The influence of the A-CNT content on the dynamic mechanical properties, mechanical properties, hardness, electrical properties, and antistatic properties was investigated.

EXPERIMENTAL

Materials

The MWCNTs used in this study were thermal chemical vapor deposition materials with a diameter of 15 nm obtained from ILJIN Nanotech Co., Ltd., in Seoul, Korea. Nitric acid (Sigma, Milwaukee, WI), hydrofluoric acid (Sigma), dibutyl tin dilaurate (Aldrich Chemical, Milwaukee, WI), and methanol (Sigma) were used without further purification. Isophorone diisocyanate (Aldrich Chemical), triethylamine (Sigma), ethylenediamine (Aldrich Chemical), methyl ethyl ketone (Sigma), and *N*-methyl-2-pyrrolidone (Aldrich Chemical) were used after dehydration with 4-Å molecular sieves for 1 day. Poly(tetramethylene oxide) glycol (number-average molecular weight = 2000 g/mol, Aldrich Chemical) was dried over calcium hydride at room temperature for 24 h. Dimethylol propionic acid (Aldrich Chemical) was dried in a vacuum oven for 5 h at 100°C.

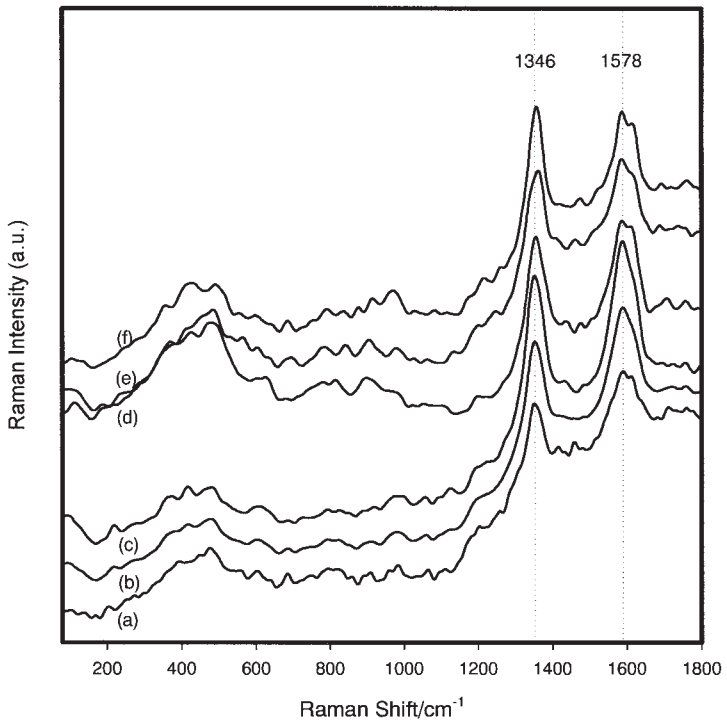

Figure 1 Raman spectra of CNT treated with nitric acid for various times: (a) 0, (b) 0.2, (c) 0.5, (d) 1, (e) 10, and (f) 24 h.

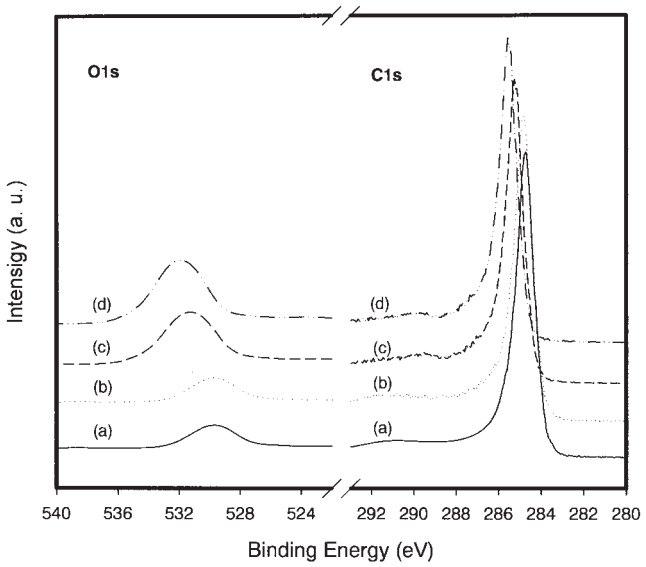

Figure 2 XPS C1s and O1s core-level scan spectra of the CNTs treated with nitric acid for various times: (a) 0, (b) 0.5, (c) 10, and (d) 24 h.

Purification and acid treatment of CNTs

To eliminate impurities such as graphite nanoparticles, carbon black and catalysts in raw CNTs (ILJIN Nanotech) were washed by the following process: the raw CNTs were washed with 20% hydrofluoric acid for 5 h and 22% nitric acid for a period of 10 h and then subsequently washed with distilled water until the pH of the CNTs approached 7. The washed CNTs were treated with boiled concentric nitric acid for a period of 0.5 h, and the A-CNTs were washed with distilled water and acetone.

Synthesis of WBPU

WBPU was synthesized by a polyaddition reaction with isophorone diisocyanate, poly(tetramethylene oxide) glycol, dimethylol propionic acid, ethylenediamine, and triethylamine. The composition and solid content of the WBPU used in this study is given in Table I. The preparation method of the WBPU is described in our previous articles.[25–29]

Preparation of the WBPU/A-CNT nanocomposites and their films

To improve the dispersability of A-CNTs into the WBPU aqueous dispersion, an A-CNT aqueous dispersion was prepared. Also, to obtain a finely dispersed A-CNT aqueous dispersion, we performed an ultrasonic treatment for 1 h at room temperature. WBPU/A-CNT nanocomposites were prepared by the mixture of the WBPU dispersion and aqueous A-CNT dispersion with magnetic stirring for 2 h, and subsequently, this was treated with ultrasonic vibration for 1 h at room temperature. The weight ratios of the WBPU/A-CNT nanocomposites were 99.99/0.01–98.5/1.5. Films for testing were prepared by the dispersions being cast onto a Teflon disk under ambient conditions. The nanocomposite films were allowed to dry at 50°C for about 1 day, and then, the remaining moisture was removed at 60°C under 20 mmHg for 2 days.

Characterization

To obtain Raman spectra of the raw CNTs and A-CNTs with a Jasco 2100 NRS spectrophotometer (Tokyo, Japan), an excitation wavelength of a 514-nm line from an argon laser was used. X-ray photoelectron spectroscopy (XPS) spectra were measured with an ESCA 250 X-ray photoelectron spectrometer (Bell Lane, East Sussex, UK) with Al Kα (1486.6 eV). The static contact angle toward distilled water was measured with a goniometer (Erma contact angle meter, Tokyo, Japan) with a water droplet (15 mm^3). The mean particle size of the raw CNTs and A-CNTs were determined with laser-scattering equipment (Autosizer, IIC, Melvern Instrument Ltd., Worcestershire, UK). The thermal dynamic mechanical behavior of the WBPU and WBPU/A-CNT nanocomposite films was measured at 4 Hz with a dynamic mechanical thermal

TABLE II
Chemical Composition of the CNTs Determined by XPS Analysis and Contact Angle towards Distilled Water of the CNTs Samples

Nitric acid treating time of CNTs (h)	Atomic %		O/C	–C–O/–C=C[a]	Contact Angle (°)
	C	O			
0	98.0	2.0	0.02	0.15	15
0.2	—	—	—	—	7
0.5	96.5	3.5	0.04	0.19	5
1	—	—	—	—	0
10	92.9	7.1	0.08	0.27	0
24	90.3	9.7	0.11	0.65	0

[a] Analyzed from C1s core-level scan spectra (XPS).

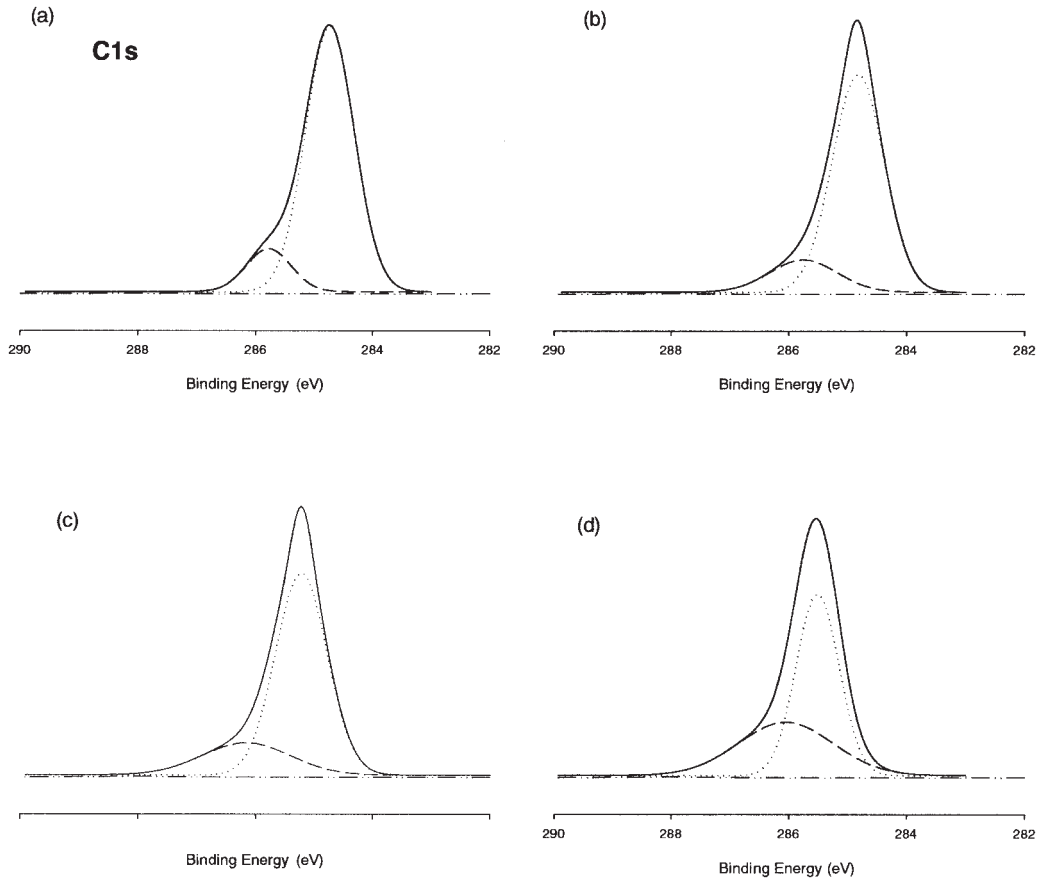

Figure 3 Curve fitting of the XPS C1s spectra of the CNTs treated with nitric acid for various times: (a) 0, (b) 0.5, (c) 10, and (d) 24 h.

analyzer (DMTA MK III, Rheometrics Scientific, Inc., Surrey, UK) with a heating rate of 3°C/min. The dimension of the film sample was 5 × 5 × 0.2 (mm) for dynamic mechanical thermal analysis measurement. The mechanical measurements were made in simple extension on dumbbell specimens with a tensile tester (Tinius Olsen 1000, PA) at a crosshead speed of 20 mm/min according to ASTM D 412. The values quoted were the averages of 10 tests. Electrical conductivity of the raw CNTs, A-CNTs, and WBPU/A-CNT nanocomposite films were measured with a surface resistance detector (CMT-SR1000N, CM Co., Ltd., Kyonggi, Korea) and the usual four-probe method. The antistatic properties of the prepared nanocomposite samples was measured with a static honestometer (Shishido Co., Ltd., Tokyo, Japan). The morphology of the WBPU/A-CNT nanocomposite films was observed by scanning electron microscopy (SEM; Hitachi S-4200 field emission scanning electron microscope, Hitachi, Ltd., Tokyo, Japan).

RESULTS AND DISCUSSION

Characterization of A-CNTs

Figure 1 shows the Raman spectra of the raw CNT and A-CNT powder measured with a highly sensitive confocal microprobe Raman system with a 514-nm line from an argon ion laser as excitation. As shown in the spectra, the raw-CNT and A-CNT samples showed well-defined Raman bands at 1578 and 1346 cm^{-1}. The position of the first strong peak at 1578 cm^{-1} was due

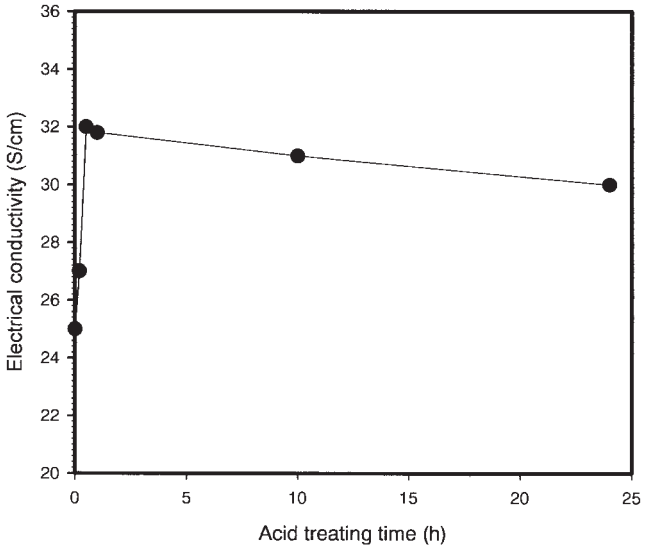

Figure 4 Electrical conductivity of the CNTs as a function of acid treatment time.

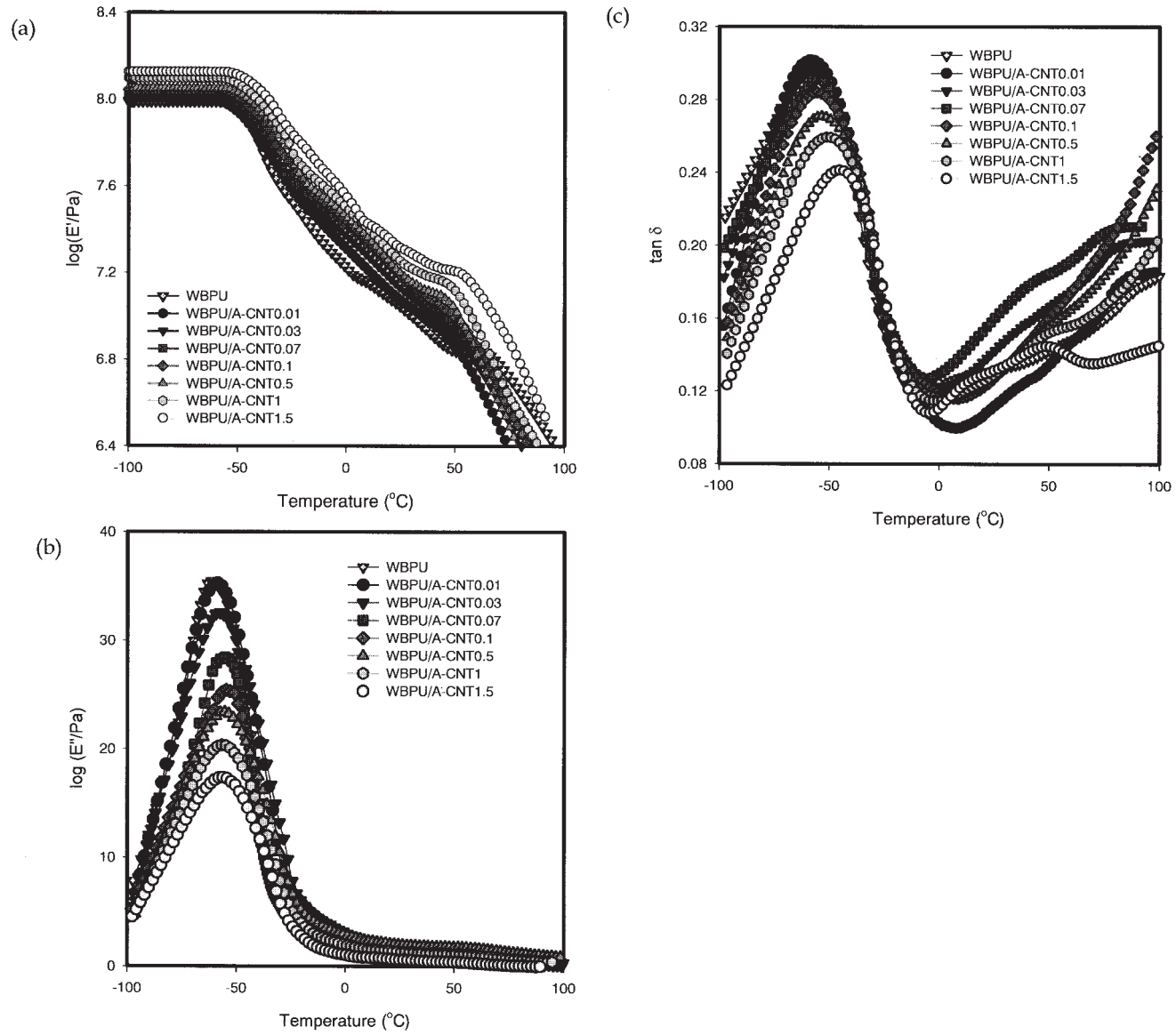

Figure 5 (a) E', (b) E'', and (c) tan δ temperature dependence on the WBPU film and WBPU/A-CNT nanocomposite films.

to the Raman-active E_{2g} mode (G-band stretching), analogous to that of graphite.[5,8,30–35] The second strong band at 1346 cm^{-1} was reasonably assigned to the D band described in the literature,[5,8,30–35] which was caused by the induction of significant defects or disorder in these nanostructures.[5,8,30–35] The frequency, intensity, and line width of the bands at 1578 and 1346 cm^{-1} of the A-CNTs were similar to those of typical CNTs. The intensity of the D band increased with increasing acid treatment time. However, the intensity of the G band significantly increased with increasing acid treatment time up to 30 min and then decreased and broadened slightly. This means that the disordered graphitic portion increased a little after 0.5 h of acid treatment.

Generally, electron spectroscopy for chemical analysis provides qualitative and quantitative information about the elemental composition of matter; particularly, it is very useful for the characterization of a polymer surfaces.[36,37] Figure 2 shows the C1s and O1s spectra of the CNTs treated with nitric acid for various times. The XPS C1s spectrum of the raw CNT exhibited a sharp peak at 284.3 eV, which was assigned to an sp^2 carbon.[36–41] The XPS O1s spectrum of the raw CNT showed a peak near 539 eV, corresponding to the —C—O—, ether-type group with oxygen singly bonded to carbon.[36,38–41] The chemical composition and O/C area ratio determined by the XPS are listed in Table II. The sp^2 peak significantly shifted to a high-binding-energy region with increasing acid treatment time. The intensity of the O1s peak increased, and its binding energy shifted toward a higher binding energy with acid treatment time. These shifts suggested that the surfaces of the CNTs were slightly

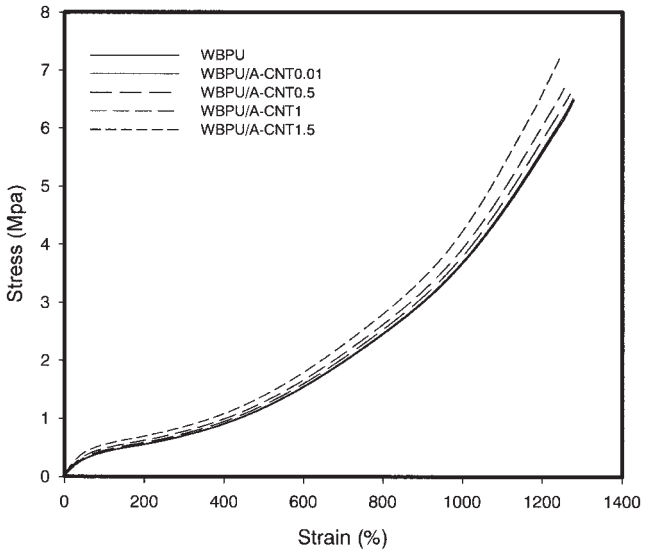

Figure 6 Stress–strain curves of (a) the WBPU film and the (b) WBPU/A-CNT0.01, (c) WBPU/A-CNT0.5, (d) WBPU/A-CNT1, and (e) WBPU/A-CNT1.5 nanocomposite films.

oxidized.[38] Figure 3 shows the curve fitting of C1s for A-CNTs treated with acid for various times. The —C—O/—C═C ratios obtained from the curve-fitting area are given in Table II. The fitting of the peaks with two Gaussian peaks indicated an sp^2 carbon (284.3 eV) and oxygen-related peaks (285–290 eV).[36–41] The atomic concentration of oxygen for raw CNT was about 2 atomic %. With increasing acid treatment time of the CNTs, the atomic concentration of carbon decreased from 98 to 90.3 atomic %. However, those of oxygen increased from 2 to 9.7 atomic %. The ratios of oxygen to carbon on the A-CNT surface increased with increasing acid treatment time, indicating the incorporation of polar groups having oxygen.

Table II also shows the results of the water contact angles of the raw CNT and A-CNT pellet samples with various acid treatment times. The water contact angles of the CNT samples significantly decreased from 15 to 0° with acid treatment time from 0 to above 1 h, which suggested an improvement in the hydrophilicity of CNTs by treatment of concentric nitric acid.

Figure 4 shows the relationship between the electrical conductivity and acid treatment time of the CNTs. The electrical conductivity of the raw CNTs was 25 S/cm. The electrical conductivity of purified A-CNTs increased with increasing acid treatment time up to 30 min and then decreased a little. The increase in the electrical conductivity might have been due to the decrease in impure materials on the A-CNT surface by acid treatment up to 30 min, whereas the decrease in electrical conductivity after 30 min of nitric acid treatment was presumably due to band gap enlargement and damage of the side wall of the CNTs.[18]

The particle size of the raw CNTs and A-CNTs was determined with laser-scattering equipment. The mean particle size of the raw CNTs and A-CNTs were 404.2 and 17.2 nm, respectively. The mean particle size of the A-CNTs was smaller than that of raw CNT. This indicates that the acid treatment led to a reduced agglomeration of CNTs.[14]

From the results of Raman analysis, XPS analysis, electrical conductivity, and mean particle size, the optimum condition of acid treatment time for the CNTs was found to be about 30 min at room temperature. Therefore, we used the A-CNTs treated with concentric nitric acid for 30 min at room temperature to prepare the WBPU/A-CNT nanocomposite materials in this study. The A-CNTs were dispersed in the WBPU matrix by ultrasonic vibration treatment.

Properties of the nanocomposites

Figure 5 shows the temperature dependence of the dynamic storage modulus (E'), loss modulus (E''), and loss tangent (tan δ) of the WBPU film and WBPU/A-CNT nanocomposite films. Jin et al.[10] reported that the enhanced E' of a MWCNT/poly(methyl methacrylate) nanocomposite was induced from the stiffening effect of the CNTs. E' of the WBPU/A-CNT nanocomposite films prepared in this study increased with increasing A-CNT content, which was due to the stiffening effect of the A-CNTs. E' values of the nanocomposite samples in the glassy plateau region significantly increased with increasing A-CNT amount, whereas the E'' peak intensity of the nanocomposite samples decreased with increasing A-CNT content. The WBPU/A-CNT nanocomposite samples had two tan δ peaks

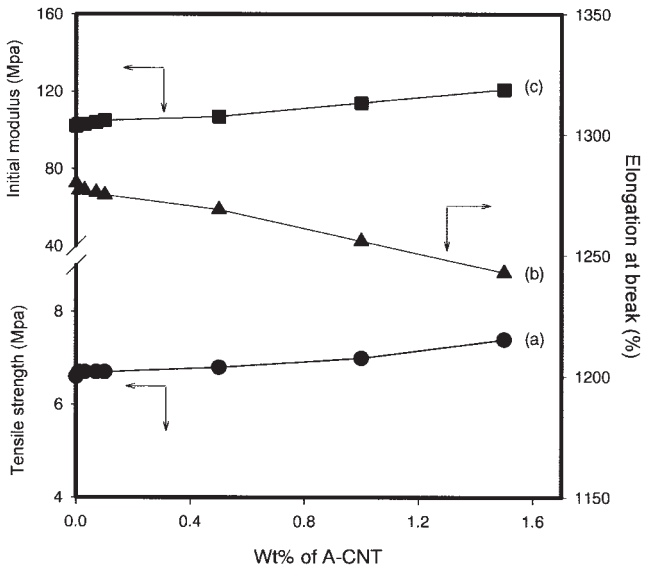

Figure 7 Effect of the A-CNT content on (a) tensile strength, (b) elongation at break, and (c) initial tensile modulus of the WBPU/A-CNT nanocomposite films.

TABLE III
Designation, Composition, Electrical Properties, Mechanical and Dynamic Mechanical Properties of WBPU/A-CNT Nanocomposite Samples

Sample designation	Composition (wt%) WBPU/A-CNT	Electrical conductivity (S/cm)	Half-life time of electrostatic charge ($\tau_{1/2}$, sec)	Tensile strength (Mpa)	Initial tensile modulus (Mpa)	Elongation at break (%)
WBPU	100/0	2.5×10^{-12}	110	6.6	102	1280
WBPU/A-CNT0.01	99.99/0.01	1.1×10^{-10}	79	6.7	103	1277
WBPU/A-CNT0.03	99.97/0.03	5.7×10^{-9}	53	6.7	103	1277
WBPU/A-CNT0.07	99.95/0.05	6.1×10^{-8}	35	6.7	104	1276
WBPU/A-CNT0.1	99.90/0.10	3.3×10^{-7}	22	6.7	105	1275
WBPU/A-CNT0.5	99.50/0.50	6.1×10^{-6}	9	6.8	107	1269
WBPU/A-CNT1	99.00/1.00	5.7×10^{-5}	5	7.0	114	1256
WBPU/A-CNT1.5	97.50/1.50	1.2×10^{-4}	1	7.4	121	1243

near −50°C assigned to the glass-transition temperature of the soft segments of WBPU and multiple tan δ peaks at higher temperatures assigned to the glass-transition temperature of the amorphous hard segments of WBPU. With increasing A-CNT content, the glass-transition temperature of the soft segments of the WBPU/A-CNT nanocomposite films shifted from −58 to −39.1°C. This means that A-CNTs were compatible with the amorphous regions of the soft segments in WBPU.

Figure 6 shows the stress–strain curves of the WBPU film and WBPU/A-CNT nanocomposite films. The results of initial modulus, tensile strength, and elongation at break of the WBPU/A-CNT nanocomposite films are summarized in Figure 7 and Table III. The initial tensile modulus, tensile strength, and elongation at break of the WBPU film were 102 MPa, 6.6 MPa, and 1280%, respectively. The initial tensile modulus and tensile strength of the nanocomposite films with 1.5 wt % loading of A-CNTs were enhanced by about 19 and 12%, respectively, compared to the corresponding values for the original WBPU film. As the A-CNT content increased from 0 to 1.5 wt %, the initial tensile modulus and tensile strength of the WBPU/A-CNT nanocomposite films increased from 102 to 121 MPa and from 6.6 to 7.4 MPa, respectively; however, the elongation at break decreased from 1280 to 1243%. These increases in the WBPU/A-CNT nanocomposite were due to the reinforcing effect of A-CNTs in the WBPU matrix.

Generally, hardness reflects the resistance to local properties and is related to crosslink density, plasticity/elasticity, strength/modulus and porosity of the matrix.[25–29] Figure 8 illustrates the dependence of hardness on the A-CNT content for the WBPU/A-CNT nanocomposite films. The hardness of the WBPU/A-CNT nanocomposite films increased with increasing A-CNT content. The increase in hardness was presumably due to the reinforcing effect of A-CNTs, as mentioned previously.

Figure 9 shows the electrical conductivity of the WBPU/A-CNT nanocomposite films as a function of the A-CNT content. The electrical conductivities of the WBPU film and A-CNT pellets were 2.5×10^{-12} and 32 S/cm, respectively. The electrical conductivity of the WBPU/A-CNT nanocomposite films increased with increasing A-CNT content. Up to 1.5 wt %, the conductivity increased by approximately eight orders of magnitude from 2.5×10^{-12} to 8.0×10^{-4} S/cm. This indicated that the conducting path, that is, the conducting network in the WBPU/A-CNT nanocomposite system, increased remarkably with increasing A-CNT content.

Figure 10 shows the antistatic half-life ($\tau_{1/2}$) and maximum surface electrostatic potential (V_{max}) of the WBPU/A-CNT nanocomposite films as a function of the A-CNT content. The values of V_{max} and $\tau_{1/2}$ of the nanocomposites prepared in this study are given in Table III. V_{max} and $\tau_{1/2}$ for the WBPU film were 57 kV

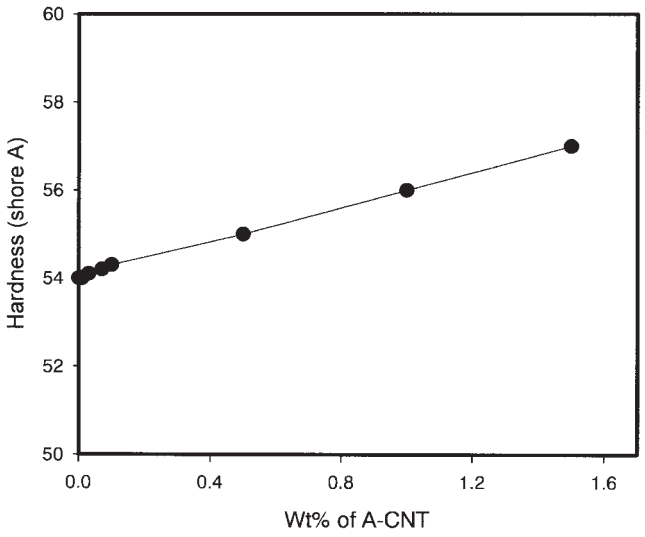

Figure 8 Effect of the A-CNT content on the hardness of the WBPU/A-CNT nanocomposite films.

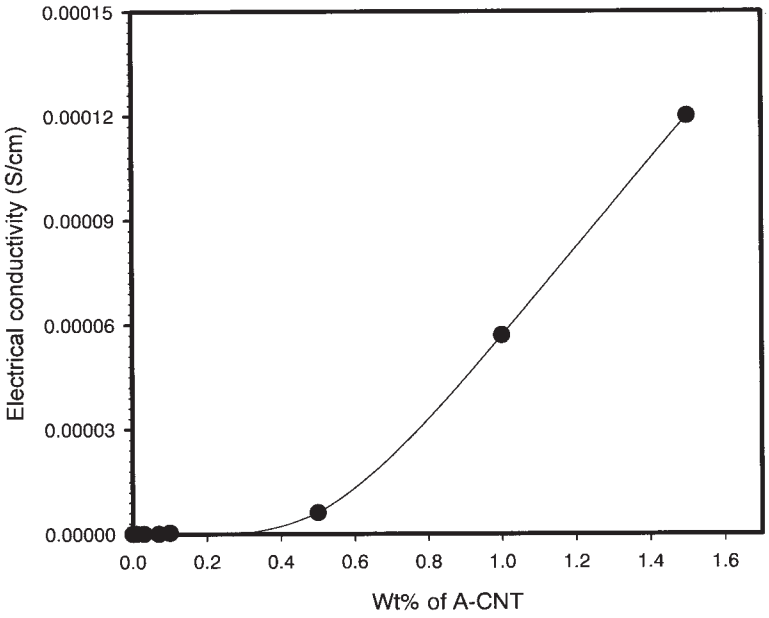

Figure 9 Effect of the A-CNT content on the electrical conductivity of the WBPU/A-CNT nanocomposite films.

and 110 s, respectively, indicating that the WBPU was a typical electrostatic material. With increasing A-CNT content from 0.01 to 1.5 wt %, the V_{max} and $\tau_{1/2}$ decreased exponentially. Generally, polymers with a $\tau_{1/2}$ lower than 10 s are considered to have good antistatic properties.[42] The WBPU/A-CNT0.5, WBPU/A-CNT1, and WBPU/A-CNT1.5 samples containing 0.5, 1, and 1.5 wt % of A-CNTs, which had $\tau_{1/2}$'s of 9, 5, and 1 s, were good antistatic materials.

SEM photographs of the fracture surfaces of the WBPU/A-CNT0.5 and WBPU/raw CNT0.5 composite films are given in Figure 11. There was no naked A-CNT fiber on the fracture surface of the WBPU/A-

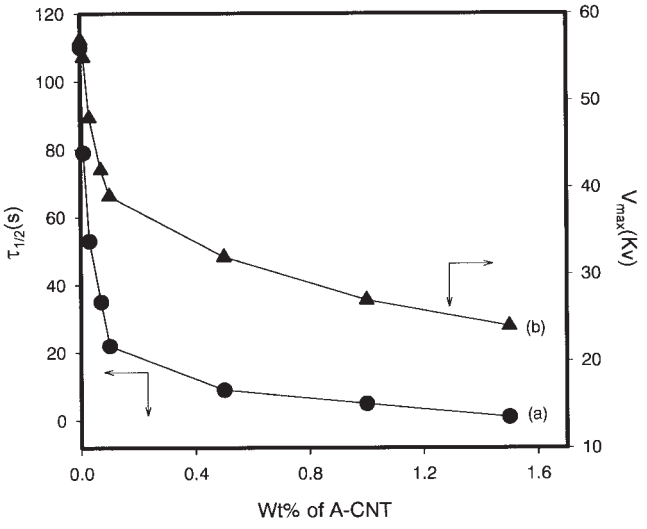

Figure 10 Effect of the A-CNT contents on the antistatic properties of the WBPU/A-CNT nanocomposite films: (a) $\tau_{1/2}$ (s) and (b) V_{max} (kV).

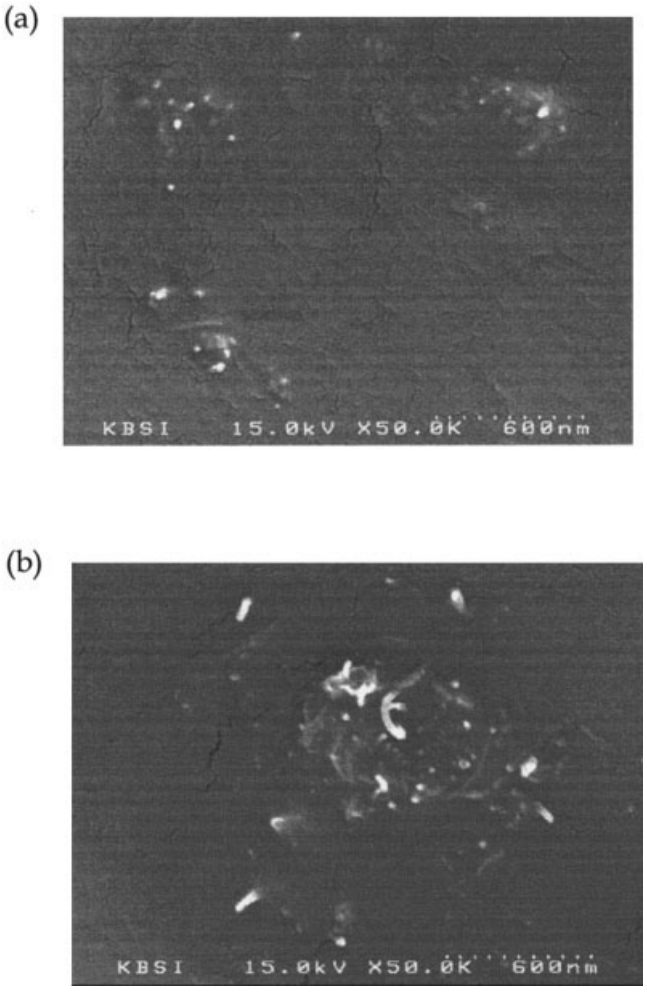

Figure 11 SEM photographs of the (a) WBPU/A-CNT0.5 and (b) WBPU/raw CNT0.5 composite films.

CNT0.5 nanocomposite [see Fig. 11 (a)], which demonstrated that A-CNT was well dispersed in the WBPU matrix. However, the aggregation and pull-apart shape of the raw CNTs appeared in the fracture surface of the WBPU/raw CNT0.5 composite [see Fig. 11 (b)]. The aggregation behavior increased with increasing A-CNT content, indicating an increase in the incompatibility of the WBPU/A-CNT composites with increasing A-CNT content.

CONCLUSIONS

A-CNTs were used as reinforcement for a WBPU/A-CNT nanocomposite. Nanocomposites of WBPU/A-CNT with various weight ratios (99.99/0.01–98.5/1.5) were prepared by solution blending/casting. WBPU/A-CNT nanocomposites with a few weight percentage loading of A-CNTs yielded material with enhanced initial tensile moduli, tensile strengths, thermal properties, electrical properties, and antistatic properties compared to the original WBPU film.

The Raman spectra of the raw CNT and A-CNT powder had well-defined Raman bands at 1578 cm^{-1} (G band) and 1346 cm^{-1} (D band). The intensity of G band significantly increased with increasing acid treatment time up to 30 min and then decreased and broadened slightly. The intensity of the D band increased with increasing acid treatment time. By XPS analysis, the intensities of C1s and O1s significantly shifted to a high-binding-energy region with increasing acid treatment time. The ratios of oxygen to carbon at the surface increased with increasing acid treatment time. In addition, as shown by the contact angle measurements, the hydrophilicity of the raw CNT was improved by concentric nitric acid treatment. The electrical conductivity of the raw CNTs was 25 S/cm. The electrical conductivity of the purified A-CNTs increased remarkably with increasing acid treatment time up to 30 min and then decreased a little. The mean particle size of the A-CNTs (17.2 nm) was smaller than that of the raw CNTs (404.2 nm).

An increase in the glass-transition temperature of the WBPU/A-CNT nanocomposites was observed, indicating that WBPU was compatible with the A-CNTs. The initial tensile modulus and tensile strength of the WBPU/A-CNT nanocomposite films increased with increasing A-CNT content. There were improvements of about 19 and 12% over WBPU in initial tensile modulus and tensile strength, respectively. The elongation at break of these nanocomposite samples decreased a little with increasing A-CNT content. The hardness of these nanocomposite films increased with increasing A-CNT content. The electrical conductivity of the WBPU film was 2.5×10^{-12} S/cm, indicating that the WBPU was a typical insulating polymer. The WBPU/A-CNT nanocomposite films exhibited significant conductivity enhancement (eight orders of magnitude) at a very low A-CNT loading (1.5 wt %). The $\tau_{1/2}$ of pure WBPU film was about 110 s, indicating that WBPU was a typical electrostatic material. However, with increasing A-CNT content from 0.01 to 1.5 wt %, $\tau_{1/2}$ and V_{max} of the WBPU/A-CNT nanocomposite films exponentially decreased. The WBPU/A-CNT1.5 sample, containing 1.5 wt % of A-CNT and with a $\tau_{1/2}$ of 1 s, had good antistatic properties.

The WBPU/A-CNT nanocomposites prepared in this study will be potentially useful in variety of coating applications because they have enhanced electrical and mechanical properties.

References

1. Ijima, S. Nature 1991, 354, 56.
2. Treacy, M. M. J.; Ebbesen, T. W.; Gibson, J. M. Nature 1996, 381, 678.
3. Wong, E. W.; Sheehan, P. E.; Lieber, C. M. Science 1997, 277, 1971.
4. Salvetat, J. P.; Kulik, A. J.; Bonard, J. M.; Briggs, G. A. D.; Stockli, T.; Metenier, K.; Bonnamy, S.; Beguin, F.; Burnham, N. A.; Forro, L. Adv Mater 1999, 11, 161.
5. Ruan, S. L.; Gao, P.; Yang, X. G.; Yu, T. X. Polymer 2003, 44, 5643.
6. Tang, W.; Santare, M. H.; Advani, S. G. Carbon 2003, 41, 2779.
7. Gordeyev, S. A.; Macedo, F. J.; Ferreira, J. A.; Hattum, F. W. J.; Bernardo, C. C. Phys B: Condens Matt 2000, 279, 33.
8. Chapelle, M. L.; Stephan, C.; Nguyen, T. P.; Lefrant, S.; Journet, C.; Bernier, P.; Munoz, E.; Benito, A.; Maser, W. K.; Martinez, M. T.; Fuente, G. F.; Guillard, T.; Flaant, G.; Alvarez, L.; Laplaze, D. Synth Met 1999, 103, 2510.
9. Jia, Z.; Wang, Z.; Xu, C.; Liang, J.; Wei, B.; Wu, D.; Zhu, S. Mater Sci Eng A 1999, 271, 395.
10. Jin, Z.; Pramoda, K. P.; Xu, G.; Goh, S. H. Chem Phys Lett 2001, 337, 43.
11. Andrews, R.; Jaques, D.; Rao, A. M.; Rantell, T.; Derbyshire, F.; Chen, Y.; Chen, J.; Haddon, R. C. Appl Phys Lett 1999, 75, 1329.
12. Schadler, L. S.; Ciannaris, S. C.; Ajayan, P. M. Appl Phys Lett 1998, 73, 3842.
13. Park, J. M.; Kim, D. S.; Lee, J. R.; Kim, T. W. Mater Sci Eng C 2003, 23, 971.
14. Gojny, F. H.; Nastalczyk, J.; Roslaniec, Z.; Schulte, K. Chem Phys Lett 2003, 370, 820.
15. Quan, D.; Dickey, E. C.; Andrews, R.; Rantell, T. Appl Phys Lett 2000, 76, 2868.
16. Jung, M.; Cho, J. W. J Korean Fiber Soc 2004, 41, 73.
17. Nalwa, H. S. Handbooks of Nanostructured Materials and Nanotechnology; Academic: San Diego, 1994; Vol.5, p 399.
18. Nalwa, H. S. Encyclopedia of Nanoscience and Nanotechnology; American Scientific: 1996; Vol. 5, p 619.
19. Kaiser, A. B.; Dusberg, G.; Foth, S. Phys Rev B 1998, 57, 1418.
20. Coleman, J. N.; Curran, S.; Dalton, A. B.; Davey, A. P.; McCarthy, B.; Blau, W.; Barklie, R. C. Phys Rev B 1998, 58, 7492.
21. Chen, J.; Harmon, M. A.; Hu, H.; Chen, Y.; Rao, A. M.; Eklund, P. C.; Haddon, R. C. Science 1998, 282, 95.
22. Mickelson, E. T.; Huffman, C. B.; Finzler, A. G.; Smalley, R. E.; Hauge, R. H.; Margrave, J. L. Chem Phys Lett 1998, 296, 188.
23. Bahr, J. L.; Tour, J. M. Chem Mater 2001 13, 3823.
24. Park, C.; Ounaies, Z.; Watson, K. A.; Crooks, R. E.; Smith, J.; Lowther, S. E.; Connell, J. W.; Siochi, E. J.; Harrison, J. S.; Clair, T. L. Chem Phys Lett 2002, 364, 303.
25. Kwon, J. Y.; Koo, Y. S.; Kim, H. D. J Appl Polym Sci 2004, 93, 700.
26. Kwon, J. Y.; Kim, E. Y.; Kim, H. D. Macromol Res, 2004, 12, 303.
27. Yang, J. E.; Kong, J. S.; Park, S. W.; Lee, D. J.; Kim, H. D. J Appl Polym Sci 2002, 86, 2375.

28. Kwak, Y. S.; Kim, H. D. Fibers Polym 2002, 3, 153.
29. Kwak, Y. S.; Park, S. W.; Lee, Y. H.; Kim, H. D. J Appl Polym Sci 2003, 89,123.
30. Chapelle, M. L.; Lefrant, S.; Journet, C.; Maser, W.; Bernier, P.; Loiseau, A. Carbon 1998, 36, 705.
31. Valentini, L.; Armentano, I.; Biagiotti, J.; Marigo, A.; Snatucci, S.; Kenny, J. M. Diamond Relat Mater 2004, 13, 250.
32. Kasuya, A.; Sasski, Y.; Saito, Y.; Tojhi, K.; Nishina, Y. Phys Rev Lett 1997, 78, 4434.
33. Eklund, P. C.; Holden, J. M.; Jishi, R. A. Carbon 1995, 33, 959.
34. Hiura, H.; Ebbesen, T. W.; Takagi, K.; Takahashi, H. Chem Phys Lett 1993, 202, 509.
35. Zhang, H. B.; Lin, G. D.; Zhou, Z. H.; Dong, X.; Chen, T. Carbon 2002, 40, 2429.
36. Skoog, D. A.; Holler, F. J. Principles of Instrumental Analysis, 5th ed.; Saunders: Philadelphia, 1992.
37. Kim, E. Y.; Kong, J. S.; An, S. K.; Kim, H. D. J. Adhes Sci Technol 2000, 14, 1119.
38. Ogasawara, T.; Ishida, Y.; Ishikawa, T.; Yokota, R. Nanocomposites Part A: Appl Sci Manufacturing 2004, 35, 67.
39. An, K. H.; Heo, G. H.; Jeon, K. G.; Bae, D. J.; Jo, C. S.; Yang, C. W.; Park, C. Y.; Lee, Y. H.; Lee, Y. S.; Chung, Y. S. Am Inst Physics 2002, 80, 4235.
40. Makris, D.; Giorgi, R.; Lisi, N.; Pilloni, L.; Salernitano, E.; Sarto, F.; Alvisi, M. Diamond Rel Mater 2004, 13, 305.
41. Valentini, L.; Canntalini, C.; Lozzi, L.; Armentano, I.; Kenny, J. M.; Santucci, S. Mater Sci Eng C 2003, 23, 523.
42. Omastova, M.; Chodak, I.; Pionteck, J. Synth Met 1999, 102, 1251.